Journal of Manufacturing Processes 32 (2018) 754–762

Contents lists available at ScienceDirect

Journal of Manufacturing Processes

journal homepage: www.elsevier.com/locate/manpro

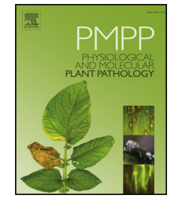

Stereo analysis on the keyhole and weld pool behaviors in K-PAW with triple CCD cameras

C.B. Jia[a,b,c,*], X.F. Liu[b,c,d], C.S. Wu[b,c], S.B. Lin[a]

[a] State Key Laboratory of Advanced Welding and Joining, Harbin Institute of Technology, Harbin 150001, China
[b] MOE Key Lab for Liquid-Solid Structure Evolution and Materials Processing, Shandong University, Jinan, 250061, China
[c] Institute of Materials Joining, Shandong University, Jinan, 250061, China
[d] Shandong College of Electronic Technology, Jinan, China

ARTICLE INFO

Keywords:
Keyhole
Weld pool
Visual sensing
Stereo analysis
K-PAW

ABSTRACT

A synchronous visual sensing system was established to observe the topside weld pool, keyhole entrance and keyhole exit at the same time during keyhole plasma arc welding (K-PAW). Complete topside weld pool was captured by a common CCD camera perpendicularly to the welding direction. Meanwhile another two cameras were employed to monitor the keyhole entrance from the rear view and to capture the keyhole exit from the substrate backside, respectively. The evolution process of the weld pool and keyhole behaviors and shapes along with the heat input accumulation were observed. The mechanism of the interactions were discussed and analyzed. Image registration was conducted fusing the weld pool, keyhole entrance and keyhole exit in the same coordinate system. The geometrical dimensions were measured and could reflect the interior intense interactions. Comprehensive investigation of the complicated physical process provided some fundamental and profound understandings.

1. Introduction

Automatic welding processes with high penetration, high efficiency and high quality have been one of the most important research subjects. Keyhole plasma arc welding (K-PAW) could penetrate medium-thickness substrates with a keyhole throughout the weld pool. This makes it have the capability to join two plates in one pass without any groove [1–2]. The main drawback of this technology is the very narrow ranges of suitable parameters to acquire high quality joints because of the vulnerability of keyhole. Robust and reliable sensing and control of the keyhole status has been the critical and indispensable task to improve the welding process stability and joint quality [3].

Researchers have always been trying to predict the keyhole status as well as the penetration in real time from the topside conveniently and reliably. However, some inherent features of this technology increased the difficulty for solving this problem. For example, the highly constricted plasma arc produces strong radiation disturbances and steep intensity gradient, the torch generally has a large volume blocking the light, the plasma arc length is short between 3–8 mm, etc. Therefore, amount of indirect sensing methods were employed. Efflux plasma voltage was roughly related to the keyhole dimensions by measuring the electrical potential of the ejected plasma arc [4–5]. Acoustic signals, plasma cloud voltage, spectral radiation, etc. were also used to indirectly reflect the keyhole status and dimensions [6–9]. However, the disadvantages such as low reliability, poor accessibility and vulnerability limited their further applications.

Compared with the above mentioned indirect sensing methods, visual sensing has been considered as an advanced and direct way to obtain very rich information from the welding processes [10–11]. Yuming Zhang et al observed the topside weld pool in gas tungsten arc welding (GTAW) to determine the weld penetration [12–14]· Three-dimensional models were developed to control the weld pool surface based on the measured results [15–17]. Guangjun Zhang et al reconstructed the three-dimensional P-GMAW weld pool based acquired two-dimensional images [18]. Wilhelm G et al used a synchronous high-speed imaging and observed the arc attachment at the wire electrode, the wire melting and the behavior of the weld pool in flux-cored arc welding (FCAW) [19]. Via directly observing the dynamic behaviors of the keyhole, vapor plume, and melt pool in full penetration laser welding, Mingjun Zhang et al explored the formation mechanisms of surface underfill [20]. By passive vision, Shen Hongyuan et al tracked the seam and control the weld pool in real time in GTAW [21]. Li Wenhang et al visually monitored the rotating arc narrow gap MAG welding process and detected the sidewall edge and arc position [22].

* Corresponding author at: State Key Laboratory of Advanced Welding and Joining, Harbin Institute of Technology, Harbin 150001, China.
E-mail address: jiachuanbao@sdu.edu.cn (C.B. Jia).

https://doi.org/10.1016/j.jmapro.2018.03.026
Received 9 January 2018; Received in revised form 25 February 2018; Accepted 22 March 2018

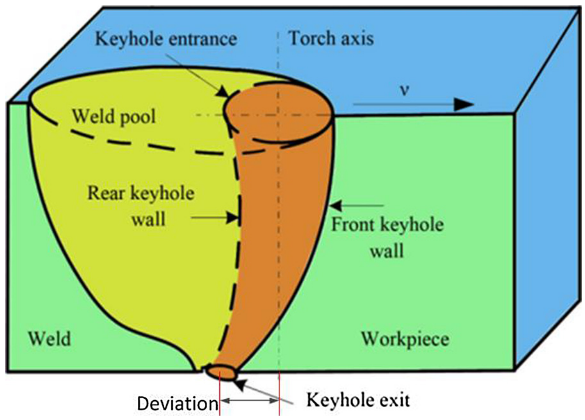

Fig. 1. The schematic diagram of keyhole entrance, weld pool and keyhole exit in K-PAW [31].

Even for submerged arc welding (SAW), Mendez P. F. et al captured the metal transfer videos at 10, 000 frames/s by inserting a thin-sheet steel tunnel perpendicular to the welding path [23].

For plasma arc welding, visual sensing is also recognized an effective way to study the complex physical processes. Wang et al observed the topside weld pool in variable polarity plasma arc welding (VPPAW) with an industrial CCD but only obtained images of partial weld pool [24]. The large-volume torch covered the welding arc and weld pool causing the invisibility of the welding area. Huijun Wang et al developed a double-side weld pool image sensor to overcome the mentioned problem [25]. Although most part of the weld pool was observed, complete weld pool images were still not obtained. Qinlian Zhang et al observed the soft variable polarity plasma arc welding process and acquired partial weld pool images with a high speed camera [26].

Because the keyhole is established through the workpiece from topside to backside, as shown in Fig. 1, it is thought that the liquid metal could be divided into 4 parts, i.e. keyhole entrance, topside weld pool, keyhole exit, backside weld pool. Apparently, it is much easier to observe the keyhole status from the backside. Y. M. Zhang and S. B. Zhang simultaneously imaged the weld pool and keyhole from workpiece backside during keyhole plasma arc welding [27]. Di Wu et al acquired the keyhole images from the back-side of the work plate in variable polarity plasma arc welding [28]. Backside keyhole, i.e. keyhole exit was monitored visually by Zuming Liu et al to study the keyhole status evolution, which was divided into 3 stages including blind stage, unstable stage and quasi-steady open keyhole stage [29]. Guokai Zhang et al further acquired the weld pool images as well as the keyhole exit images from the substrates' backside [30]. Based on the above-mentioned backside imaging, the keyhole exit and backside weld pool could be well observed and measured. However, the topside weld pool and the keyhole entrance are also very important for obtaining a high-quality weld joint and stable process. Particularly, the plasma arc acted firstly and directly on the liquid metal from the workpiece top surface. The authors used one common CCD camera and successfully acquired complete topside weld pool images [31].

Above all, the weld pool and keyhole behaviors were generally monitored, discussed and analyzed separately. Interactions between plasma arc, keyhole, topside and backside weld pool need to be investigated integrally for better understanding the complicated welding process. Xiaoxia Jian et al performed numerical investigation on the coupled interaction mechanism of the plasma arc, weld pool and keyhole in plasma arc welding. Unified governing equations were solved in the whole domain including the torch, plasma arc, keyhole, weld pool and workpiece [32]. However, references presenting captured complete weld pool and keyhole images from both topside and backside have not be found. Because the weld pool and keyhole exist in different sides of the substrate, multi rather than one CCD cameras are needed to comprehensively understand the interactions. Bračun D. and Sluga A. developed a stereo vision measuring system using two stereo cameras for an on-line welding path inspection in order to acquire information about the welding path [33]. Nomura K, Yoshii K et al used 12 CCD cameras with three types of narrow-band interference filters and built a multi-directional and heterochromatic measurement system to capture axially asymmetric plasma in MIG welding [34].

In this study, it was proposed that three CCD cameras constitute a stereo imaging system. The complete topside weld pool should be captured by one camera perpendicularly to the welding direction; another camera was used to monitor the keyhole entrance, i.e. the keyhole opening on the top; the last camera was used to monitor the keyhole exit from the substrate backside. In this case, the behaviors of the liquid metal and keyhole can be observed synchronously. Their interactions and the influences from plasma arc, gas flow, etc. were investigated and discussed.

2. Experimental setup

A synchronous visual sensing system was developed as shown in Fig. 2. The system consists of three CCD cameras, i.e. CCD 1 to monitor the topside weld pool, CCD 2 to capture the keyhole entrance, and CCD 3 to observe the keyhole exit from the substrate backside. The CCD 1 had an angle of 10 degrees from the substrate surface (α_1), 90 degrees from the welding direction, 150 mm distance and targeting at the complete weld pool laterally [35]. The CCD 2 was fixed above the substrate targeting at the rear part of the keyhole entrance with the shooting distance 180 mm and an angle of 15 degrees (α_2). The CCD 3 was amounted with a 60° angle from the substrate backside surface (α_3). Note that CCD 2 and CCD 3 cameras were in the same plane as the weld seam and welding torch.

Stainless steel plates with 6 mm thickness were bead-on-plate welded by a Fronius plasma arc welding power source with preset parameters: $I = 150$ A, $v = 120$ mm/min, tungsten electrode diameter

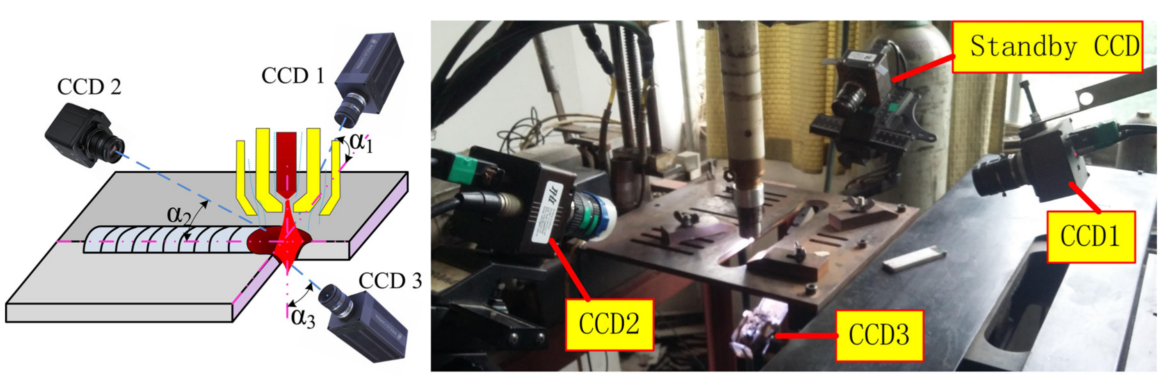

Fig. 2. Observations of the weld pool and keyhole status with triple CCD cameras.